Development/Plasticity/Repair

# Receptor Tyrosine Phosphatases Guide Vertebrate Motor Axons during Development

**Laurie Stepanek,[3,4] Andrew W. Stoker,[5] Esther Stoeckli,[6] and John L. Bixby[1,2,3,4]**

Departments of [1]Molecular and Cellular Pharmacology and [2]Neurological Surgery, [3]Neuroscience Program, and [4]Miami Project to Cure Paralysis, University of Miami School of Medicine, Miami, Florida 33136, [5]Institute of Child Health, University College London, London WC1N 1EH, United Kingdom, and [6]Institute of Zoology, University of Zurich, 8057 Zurich, Switzerland

**Receptor-type protein tyrosine phosphatases (RPTPs) are required for appropriate growth of axons during nervous system development in *Drosophila*. In the vertebrate, type IIa RPTPs [protein tyrosine phosphatase (PTP)-δ, PTP-σ, and LAR (leukocyte common-antigen-related)] and the type III RPTP, PTP receptor type O (PTPRO), have been implicated in the regulation of axon growth, but their roles in developmental axon guidance are unclear. PTPRO, PTP-δ, and PTP-σ are each expressed in chick motor neurons during the period of axonogenesis. To examine potential roles of RPTPs in axon growth and guidance *in vivo*, we used double-stranded RNA (dsRNA) interference combined with *in ovo* electroporation to knock down RPTP expression levels in the embryonic chick lumbar spinal cord. Although most branches of the developing limb nerves appeared grossly normal, a dorsal nerve identified as the anterior iliotibialis was clearly affected by dsRNA knock-down of RPTPs. In experimental embryos treated with dsRNA targeting PTP-δ, PTP-σ, or PTPRO, this nerve showed abnormal fasciculation, was reduced in size, or was missing entirely; interference with PTPRO produced the most severe phenotypes. Control embryos electroporated with vehicle, or with dsRNA targeting choline acetyltransferase or axonin-1, did not exhibit this phenotype. Surprisingly, embryos electroporated with dsRNA targeting PTP-δ together with PTPRO, or all three RPTPs combined, had less severe phenotypes than embryos treated with PTPRO alone. This result suggests that competition between type IIa and type III RPTPs can regulate motor axon outgrowth, consistent with findings in *Drosophila*. Our results indicate that RPTPs, and especially PTPRO, are required for axon growth and guidance in the developing vertebrate limb.**

*Key words:* **tyrosine phosphorylation; neurite outgrowth; motor neurons; spinal cord; chick embryo; axon guidance**

## Introduction

Receptor protein tyrosine phosphatases (RPTPs) are transmembrane proteins implicated in the regulation of axon growth and guidance (Bixby, 2000; Johnson and Van Vactor, 2003). In particular, genetic evidence implicates type IIa and type III RPTPs in pathway selection by photoreceptors, CNS axons, and motor neurons in *Drosophila* (Van Vactor et al., 1998; Newsome et al., 2000; Clandinin et al., 2001; Maurel-Zaffran et al., 2001; Schindelholz et al., 2001; Sun et al., 2001). The low penetrance of defects in RPTP null mutants, and similarities in phenotypes between null mutants of different RPTPs, suggest redundancy in RPTP function during axonogenesis. However, examination of multiple mutants indicates both cooperation and competition among RPTPs in guiding axons (Desai et al., 1997; Schindelholz et al., 2001).

Received Nov. 4, 2004; revised Feb. 8, 2005; accepted Feb. 28, 2005.

This work was supported by National Institutes of Health Grant NS38920 (J.L.B.). L.S. was a Lois Pope Leaders in Furthering Education Fellow. We thank Dr. Vance Lemmon for the L1 antibody and for helpful criticism of the manuscript, Andrew Rosendahl for the nerve branch area analysis program, and Dr. Lynn Landmesser for assistance with chick neuroanatomy. We also thank Beata Frydel and the Miami Project Core Imaging Facility for imaging help. Drs. Vlad Pekarik, Dan Liebl, and Ken Muller provided excellent technical advice. We thank Katy Reinhard for help with tissue sectioning.

Correspondence should be addressed to Dr. John L. Bixby, Miami Project to Cure Paralysis, University of Miami School of Medicine, 1095 Northwest 14th Terrace, Miami, FL 33136. E-mail: jbixby@miami.edu.

DOI:10.1523/JNEUROSCI.4531-04.2005

 0270-6474/05/253813-11$15.00/0

Evidence of RPTP function in vertebrate axon pathfinding is less clear. *In vitro* evidence links the vertebrate type IIa RPTPs leukocyte common-antigen-related (LAR), protein tyrosine phosphatase (PTP)-δ, and PTP-σ to axon growth regulation (Ledig et al., 1999b; Wang and Bixby, 1999; Q. L. Sun et al., 2000; Yang et al., 2003), and similar evidence has been obtained for the type III RPTP, PTP receptor type O (PTPRO) (Stepanek et al., 2001). Experiments using putative dominant-negative mutants of PTP-σ and PTP-δ suggest involvement of these RPTPs in pathfinding *in vivo* (Johnson et al., 2001; Rashid-Doubell et al., 2002). LAR, PTP-δ, and PTP-σ mutant mice have nervous system phenotypes, some of which may be related to axon growth (Yeo et al., 1997; Elchebly et al., 1999; Wallace et al., 1999; Uetani et al., 2000). Finally, LAR and PTP-σ null mutants exhibit aberrant peripheral nerve regeneration (Xie et al., 2001; McLean et al., 2002; Thompson et al., 2003; Van der Zee et al., 2003). Direct loss-of-function experiments linking these RPTPs to developmental axon guidance have not been reported.

The routes taken by embryonic motor axons to their targets are relatively well understood. In the chick spinal cord, axons from different motor pools are intermingled, because they grow toward a "choice point" at the base of the limb; there, axons segregate and extend dorsally or ventrally (Landmesser, 1978b; Lance-Jones and Landmesser, 1981). In the limb, axons diverge again to grow to their proper target muscles (Lance-Jones and

Landmesser, 1981; Tosney and Landmesser, 1985). Type IIa and type III RPTPs are involved in decision making at motor neuron choice points in *Drosophila*, and these functions may be conserved. Because several such RPTPs are expressed in embryonic chick motor neurons, these neurons should be a useful system for examining the roles of RPTPs in vertebrate axon guidance.

In the chick, RNA interference (RNAi) can be combined with *in ovo* electroporation to knock down expression of guidance proteins in the developing spinal cord (Pekarik et al., 2003). We used this methodology to perform loss-of-function experiments for PTP-δ, PTP-σ, and PTPRO in developing spinal motor neurons. Our studies provide the first evidence for the involvement of a vertebrate type III RPTP in axon growth *in vivo*, and support the idea of cooperation and competition among vertebrate RPTPs in regulation of motor axon pathfinding.

## Materials and Methods

*Materials.* Fertilized White Leghorn chicken eggs were purchased from SPAFAS (Norwich, CT) and incubated in a humidified incubator at 38°C until the desired stage of development. All of the chemicals were purchased from Sigma (St. Louis, MO) unless stated otherwise.

In situ *hybridization.* Plasmids containing cDNA for base pairs 382–1004 of chick (c)PTPRO (accession number U65891), base pairs 1093–1489 of cPTP-σ (accession number L32780), and a portion of cPTP-δ that aligns to base pairs 877–1478 of human PTP-δ (accession number L38929) were linearized and used as templates for transcription of sense and antisense digoxygenin-labeled riboprobes using the recommended procedure (Roche, Mannheim, Germany). Embryos were dissected at embryonic day 5.5 (E5.5), fixed in 4% paraformaldehyde overnight, cryoprotected in 30% sucrose overnight, and frozen in OCT (Tissue Tek; Fisher Scientific, Pittsburgh, PA) for cryosectioning. Ten-micrometer-thick sections were allowed to dry and processed for *in situ* hybridization following a standard protocol (Schaeren-Wiemers and Gerfin-Moser, 1993). Sections were hybridized overnight with 600 ng/ml riboprobe at 56°C.

*Production of double-stranded RNA.* Sense and antisense RNAs were produced from plasmids encoding portions of cPTP-σ (base pairs 1093–1489), cPTP-δ (aligns to base pairs 877–1478 of human PTP-δ), cPTPRO (base pairs 1458–2334), and cChAT (base pairs 1344–1665; accession number AY044155). After linearization with the appropriate restriction endonucleases, RNA was transcribed using the SP6 and T7 MegaScript kits from Ambion (Austin, TX). RNA was cleaned, analyzed, and annealed as described previously (Pekarik et al., 2003).

In ovo *RNA interference.* Double-stranded RNA (dsRNA) injection and electroporation were performed as described previously (Pekarik et al., 2003). Embryos were injected at E3 to E3.5 [Hamburger and Hamilton stages (HH) 18–20] and dissected 48–60 h later (HH 25–27). dsRNA for combinatorial RNA interference (RNAi) was injected at a final concentration of 500 ng/μl for each RNA. This gave molarities of 1.7 μM for PTP-σ, 1.1 μM for PTP-δ, 0.8 μM for PTPRO, and 2.0 μM for choline acetyltransferase (ChAT).

*Western blotting.* Embryos were dissected 48 h postelectroporation in cold PBS–glucose. The lumbosacral portions of 10–15 spinal cords were split into right and left sides and lysed in 1% Igepal CA-630, 5 mM EDTA, 100 μg/ml PMSF, 1 mg/ml leupeptin, 1 mg/ml aprotinin, and 1 mg/ml pepstatin A in TBS (25 mM Tris, 150 mM NaCl, pH 7.4) for 30 min. Undissolved pellets were cleared by centrifugation (12,000 × *g*; 30 min), and 50 μg of supernatant protein was separated on SDS-PAGE and transferred to nitrocellulose as described previously (Bixby and Jhabvala, 1990). Primary antibodies were rabbit anti-cPTPRO (Ledig et al., 1999a) at 1:2500, or rabbit anti-cPTP-σ (Stoker et al., 1995) at 1:5000. Secondary antibody was Alexa Fluor 680 goat anti-rabbit IgG (Molecular Probes, Eugene, OR). After rinsing, blots were incubated with anti-chick L1 cell adhesion molecule (L1CAM) (Lemmon and McLoon, 1986), followed by infrared dye 800-conjugated anti-mouse IgG (Rockland, Gilbertsville, PA). Bound antibody was visualized, and band intensity was quantified using the LI-COR (Lincoln, NE) Odyssey Infrared Imaging System.

*Whole-mount embryo staining.* Embryos were dissected and fixed in 4% paraformaldehyde overnight. After rinsing in PBS, embryos were incubated in 1% Triton X-100 for 1 h, followed by 20 mM lysine in 0.1 M sodium phosphate for 1 h, followed by blocking in 10% goat serum in PBS for 4 h. Embryos were incubated in anti-neurofilament-M antibody (RMO270; Zymed, San Francisco, CA) diluted 1:1500 in blocking solution for 48 h at 4°C. Embryos were rinsed overnight in PBS, and then incubated in cyanine 3 (Jackson ImmunoResearch, West Grove, PA) or Alexa Fluor 594 goat anti-mouse IgG (Molecular Probes) diluted 1:2000, for 16 h at 4°C.

*Phenotype quantification.* Embryos were categorized as unaffected or affected by experimenters blinded to treatment group. An initial subgroup, containing embryos from all single-treatment, PBS, and control groups, were analyzed separately by three experimenters and categorized by each based on comparison of the treated anterior iliotibialis (AITIB) with the untreated AITIB. Embryos were categorized as affected if there was a gross difference in morphology or nerve size between the electroporated and nonelectroporated sides, including missing nerves, severely truncated nerves, or gross changes in branching/fasciculation.

For calculation of nerve area, images of neurofilament-stained nerves were captured with a Nikon (Melville, NY) Coolpix 990 camera mounted on a Nikon Eclipse TE300 microscope. An algorithm designed in Igor Pro 4.01 (A. R. Rosendahl, University of Miami, Miami, FL) was used to analyze the images. Briefly, the algorithm used an adaptive thresholding process to extract nerve pixels from background. The same images were used for Neurolucida analysis. An experimenter traced each branch of the nerves in Neurolucida 5.04.3 (MicroBrightField, Williston, VT). This tracing was then used by Neuorexplorer 3.60.3 (MicroBrightField) to calculate branch length and the number of primary branches (defined as branching of axon bundles from the main axon fascicle) for each nerve. For all of the quantitative measures, we calculated the ratio of the measurements between treated and untreated nerve. These values were then used to compare all of the treatment groups using nonparametric ANOVA (Kruskal–Wallis test) followed by Dunn's multiple comparisons test to compare individual treatment groups.

*1,1′-Dioctadecyl-3,3,3′,3′-tetramethylindocarbocyanine perchlorate tracing.* After dissection, embryos were stored in 4% paraformaldehyde. For retrograde tracing, nitrocellulose membrane was soaked with a 1 mg/μg dimethylformamide solution of 1,1′-dioctadecyl-3,3,3′,3′-tetramethylindocarbocyanine perchlorate (DiI) (D-282; Molecular Probes) and allowed to dry. Small pieces of nitrocellulose were inserted into the limb bud in the termination zone of the AITIB. Embryos were stored at 37°C for 5 d. After tracing was complete, embryos were embedded in 6.25% agar type IX, and 250 μm transverse sections were cut on an oscillating tissue slicer (Electron Microscopy Sciences, Ft. Washington, PA). Anterograde tracing was performed on 250 μm sections cut in the same way. The untreated side of the embryo was marked with india ink. Glass capillaries with a tip diameter of ~5 μm were dipped into 5 mg/ml DiI dissolved in ethanol and placed into the ventrolateral spinal cord. After 1 h, capillaries were removed, and the sections were stored in the dark at room temperature for 7 d. Images were scanned using a Zeiss (Oberkochen, Germany) LSM510 confocal microscope (Miami Project to Cure Paralysis), and manipulated in Adobe Photoshop.

*Islet-2 staining and design-based stereology.* Embryos were dissected and fixed at 4°C for 1.5 h. Every fifth section of 20 μm cryostat sections from the rostral lumbosacral region was processed for Islet-2 (Isl-2) immunohistochemistry. The Islet-2 primary antibody (51.4H9) developed by T. M. Jessell (Columbia University, New York, NY) was obtained from the Developmental Studies Hybridoma Bank (Iowa City, IA) developed under the auspices of the National Institute of Child Health and Human Development and maintained by the University of Iowa (Iowa City, IA). Sections were incubated in a 1:100 dilution of 51.4H9 at 4°C for 48 h. After rinsing, they were incubated in a 1:1000 dilution of biotinylated anti-mouse IgG (Vector Laboratories, Burlingame, CA). Bound antibody was visualized with the Vectastain Elite ABC kit (Vector Laboratories) followed by a nickel-intensified DAB reaction. Stereo Investigator 5.05.04 (MicroBrightField) was used to estimate the number of Islet-2-positive cells through the volume of the sectioned area. DAB-positive cells were counted in the right and left ventral horns of each section using a counting frame of 25 × 25 μm and a scan grid size of 45 × 45 μm. At least 300 cells on each side were counted per embryo. From this, the

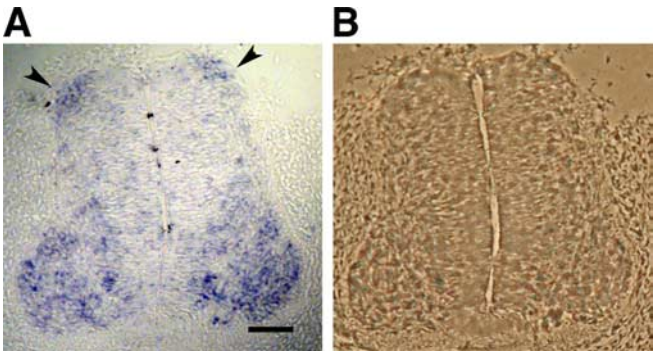


**Figure 1.** PTPRO is expressed in the ventral horn of the embryonic chick spinal cord. Bright-field (***A***) and phase-contrast (***B***) images of a cryostat section from LS 2 of E5 chick hybridized to an antisense cPTPRO riboprobe and developed with alkaline phosphatase (blue reaction product) are shown. PTPRO mRNA was concentrated in large cells in the lateral portion of the ventral horn, as well as in dorsolateral commissural neurons (arrowheads). Dorsal, Up. Scale bar, 100 $\mu$m.

software estimated upward of 5000 Isl-2-positive cells per side of each embryo in the sectioned region.

*PTPRO–GFP (green fluorescent protein) electroporation.* PCR was used to add a unique *Sal*I site at base pair 3100 just 3′ of the sequence encoding the 28-aa juxtamembrane region of cPTPRO. The entire extracellular domain, transmembrane region, and juxtamembrane region were cloned into the pEGFP-N2 vector (Clontech, Palo Alto, CA) in-frame with the GFP-coding sequence. This cPTPRO–GFP construct was released from the pEGFP vector and cloned into a modified pIRES plasmid with a $\beta$-actin promoter (Pekarik et al., 2003). PTPRO–GFP was electroporated with dsChAT RNA or dsPTPRO RNA at a final concentration of 1.5 $\mu$g/$\mu$l. After 48 h, embryos were dissected and 100 $\mu$m sections of the lumbosacral segments were cut on an oscillating tissue slicer as described above. All of the in-focus green cells were counted in each section, and at least 10 sections were examined per embryo.

*Statistics.* Statistics were done using InStat (version 2.03).

## Results

### RPTPs are expressed in the lateral motor column of the embryonic chick spinal cord

The pathways taken by chick motor axons to their targets in the hindlimb are well understood, and the motor neurons are accessible for embryonic manipulation. We therefore chose to examine regulation of motor axon growth in the chick lumbosacral spinal cord. Two type IIa RPTPs, PTP-$\delta$ and PTP-$\sigma$, and one type III RPTP, PTPRO, are expressed during the period of axon outgrowth in motor columns of the rodent spinal cord and the chick brachial spinal cord (Yan et al., 1993; Sommer et al., 1997; Chilton and Stoker, 2000; Beltran et al., 2003; Thompson et al., 2003). To determine whether these RPTPs are also expressed in chick lumbosacral motor neurons, we performed *in situ* hybridization using digoxygenin-labeled riboprobes. PTPRO mRNA was expressed in the ventral horn, including large neurons, and in the dorsolateral commissural neurons (Fig. 1) as well as in the dorsal root ganglia (data not shown) of E5 chick embryos. This is fully consistent with the pattern seen previously in the brachial spinal cord (Chilton and Stoker, 2000). PTP-$\delta$ mRNA was expressed diffusely throughout the lumbar spinal cord, including the ventral horn, and PTP-$\sigma$ mRNA was found in the ventral horn and in the ventricular zone (data not shown). This pattern of mRNA expression is consistent with our hypothesis that these three RPTPs are involved in the growth of hindlimb motor axons from the embryonic chick spinal cord.

### Electroporation of dsRNA specifically "knocks down" protein levels of target RPTP

To assess the roles of RPTPs in motor axon guidance, we used *in ovo* electroporation combined with RNAi. Electroporation of long dsRNAs has been shown to produce specific and reproducible decreases in expression of target proteins (Pekarik et al., 2003). The phenotypes resulting from gene silencing by RNAi are specific, in the sense that dsRNA targeting of known axonal guidance proteins produces the same axonal pathfinding defects as injection of cognate function-blocking antibodies, and expression levels of nontargeted proteins from the same family as the targeted protein are not changed (Stoeckli and Landmesser, 1995; Pekarik et al., 2003). Recently, *in ovo* electroporation of short interfering RNA (siRNA) hairpins was shown to successfully knock down neuropilin-1 in the chick spinal cord (Bron et al., 2004). Although this methodology is advantageous in that interfering RNA is continuously produced, using one long (400–800 bp) dsRNA allowed us to sidestep issues of sequence selection, which is important because siRNAs differ in their effectiveness (Elbashir et al., 2001; Holen et al., 2002). We produced dsRNAs targeting the type III RPTP, PTPRO, and the type IIa RPTPs, PTP-$\delta$ and PTP-$\sigma$. These dsRNAs were injected into the central canal of E3.5 chick spinal cords (HH 18–20) and electroporated into the lumbosacral region. Because the electroporation confines transfection to one side of the spinal cord (Pekarik et al., 2003) (data not shown), this side will be referred to as the "treated" side; the other side acts as a control. After electroporation, the chicks were allowed to develop for 48 h. During this time period, motor neurons extend axons into the periphery (Hamburger, 1975; Oppenheim and Heaton, 1975).

We evaluated the efficacy of gene silencing by RNAi in two ways, using PTPRO as our test protein. In an initial series of experiments, we combined *in ovo* electroporation with coinjection of (1) a plasmid encoding a GFP fusion protein containing the extracellular, transmembrane, and juxtamembrane domains of PTPRO, and (2) dsRNA targeting either PTPRO or ChAT as a control. This allowed us to use GFP fluorescence to evaluate any change in transfected PTPRO expression attributable to dsRNAi. In embryos transfected with PTPRO–GFP and dsRNA targeting ChAT, a large number of GFP-expressing cells was always observed (Fig. 2*B*). In contrast, many fewer GFP-positive cells were observed after cotransfection of dsRNA targeting PTPRO (Fig. 2*D*). This effect was quantified by counting the number of GFP-positive cells per section in the two conditions. On average, we found 18.6 $\pm$ 1.8 (mean $\pm$ SEM) green fluorescent cells per section in the embryos cotransfected with ChAT dsRNA, compared with 1.4 $\pm$ 0.3 cells per section with PTPRO dsRNA ($n = 3$ embryos in each group; $p < 0.0001$). This drastic decrease in PTPRO–GFP expression was apparent throughout the electroporated region; there was no evidence that a subset of cells was more sensitive to electroporation or RNAi.

These experiments demonstrate that our dsRNA can effectively target PTPRO, but do not resolve the extent to which endogenous PTPRO is affected. Because our cPTPRO antibody is ineffective in immunohistochemistry, we examined this issue by Western blotting. The lumbosacral spinal cords from 10–15 embryos were dissected and split into left and right halves, lysed, separated on SDS-PAGE, and probed with antibodies to RPTPs on Western blots. When we examined PTPRO expression in embryos treated with dsRNA targeting PTPRO, we found the ratio of PTPRO expression [left (or treated) side/right (or untreated) side] to be decreased by 29% relative to this ratio in untreated control embryos ($p < 0.05$) (Fig. 3). Thus, dsRNA treatment

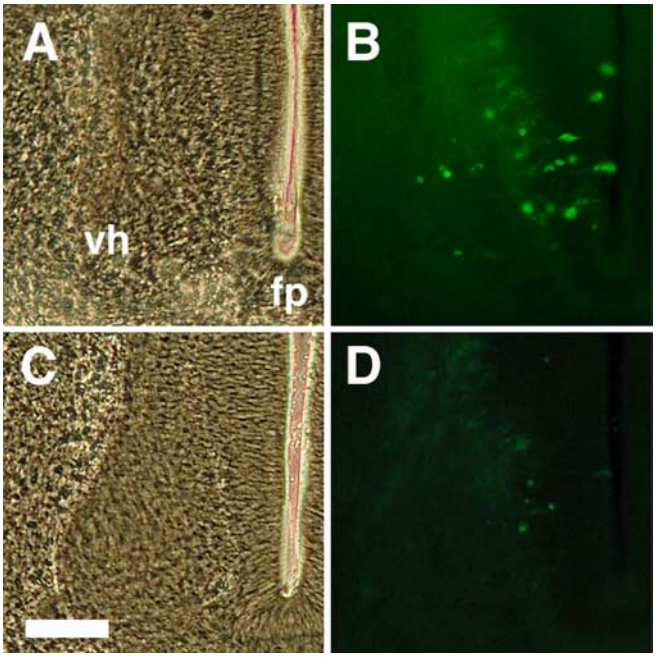


**Figure 2.** Electroporation of dsPTPRO mRNA knocks down expression of exogenous PTPRO–GFP. Spinal cords were electroporated with a cDNA encoding a PTPRO–GFP fusion protein, together with either ChAT dsRNA (***A***, ***B***) or PTPRO dsRNA (***C***, ***D***). After 48 h, transverse sections of the lumbosacral spinal cord region were examined for GFP fluorescence. Phase-contrast images of LS 2 sections from dsChAT embryos (***A***) and dsPTPRO embryos (***C***) are shown to the left of fluorescent images of the same sections (***B***, ***D***, respectively). Numerous cells expressing PTPRO–GFP are visible in the embryos treated with dsChAT mRNA (***B***) but are barely detectable in embryos treated with dsPTPRO (***D***). fp, Floorplate; vh, ventral horn. Scale bar, 100 $\mu$m.

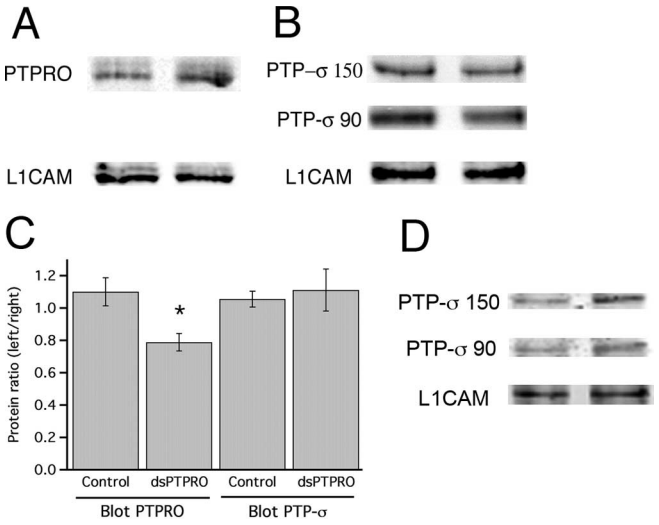


**Figure 3.** Endogenous PTPs are selectively knocked down by electroporation with dsRNA. ***A–C***, Spinal cords were electroporated with PTPRO dsRNA or left untouched (Control). At E5, lumbosacral regions of the cords were dissected into left (treated) and right (untreated) halves, and pooled, and levels of PTPRO and control proteins were examined by Western blot. ***A***, ***B***, Representative blots of spinal cord lysates from left and right sides of experimental embryos. ***A***, Blot probed with antibodies to PTPRO and to L1CAM. The PTPRO band at 180 kDa is fainter in the treated lysate, whereas the loading control (L1CAM; 90 kDa) is slightly stronger on the treated side. ***B***, Blot probed with antibodies to PTP-$\sigma$ and to L1CAM. The PTP-$\sigma$ antibody recognizes two bands: the full-length form, PTP-$\sigma$2 at 150 kDa, and PTP-$\sigma$1 at 90 kDa. These bands are approximately equal in intensity between the untreated and treated sides, as is the L1CAM band. ***C***, Band intensity was calculated using the Odyssey system. The ratio of left:right RPTP band intensity, normalized to L1CAM, is shown (mean $\pm$ SEM). Control embryos have slightly more PTPRO and PTP-$\sigma$ protein on the left side. Experimental embryos (dsPTPRO) show no change in relative PTP-$\sigma$ levels, but 21.3% less PTPRO protein on the left side. $n = 3$ for both control groups and dsPTPRO groups. *$p < 0.05$, two-tailed $t$ test comparing PTPRO group with control. ***D***, Spinal cords were electroporated with PTP-$\sigma$ dsRNA; lumbosacral regions were dissected and subjected to Western blotting with antibodies to PTP-$\sigma$ and to L1CAM. Whereas the L1 band is approximately equal in intensity on the two sides, both PTP-$\sigma$ bands are fainter on the treated (left) side. The average decrease in protein on the treated side (normalized to L1) was 25% ($n = 3$ experiments).

reduced PTPRO expression levels significantly. To evaluate the specificity of this result, we examined the relative levels of PTP-$\sigma$ on the two sides of spinal cords in control embryos and embryos treated with PTPRO dsRNA. In this case, the expression ratio was unchanged (5.5% increase; NS) (Fig. 3). Thus, there is a specific decrease of the target RPTP (PTPRO) in embryos that are electroporated with PTPRO dsRNA.

We also tested knock-down of a second RPTP using dsRNA targeting PTP-$\sigma$; knock-down of PTP-$\sigma$ protein was clearly seen in Western blots (Fig. 3). Analysis of blots from three different experiments revealed that knock-down of PTP-$\sigma$ protein averaged 25%, similar to what was seen with PTPRO dsRNA. Our results are consistent with previous experiments demonstrating specific knock-down of axonin-1 expression by the same protocol (Pekarik et al., 2003). In this study, estimated knock-down averaged 28%, quantitatively similar to the present findings with PTPRO and PTP-$\sigma$. Together, the data suggest that our RNAi protocol specifically and effectively knocks down expression of the target RPTP. Because our evaluation of PTPRO and PTP-$\sigma$ knock-down is quantitatively consistent with axonin-1 knock-down, we expect that knock-down efficiency for PTP-$\delta$ is similar; we could not test this directly because we lack a useful antibody to cPTP-$\delta$.

It is important to note that knock-down of PTPRO in transfected neurons is underestimated by our Western blot data. First, only a fraction ($\leq$60%) of the cells on the treated side are transfected (Pekarik et al., 2003). Thus, knock-down in transfected cells must be at least 50%. Second, by using the entire hemicord over the entire lumbosacral region, we are including tissue not likely to be efficiently electroporated. Finally, PTPRO is present in axons and growth cones (Bodden and Bixby, 1996; Stepanek et al., 2001), and our samples will therefore contain axonal protein from neurons outside the targeted area. It is difficult to estimate the magnitude of the latter two effects, but our results with PTPRO-GFP suggest that knock-down is likely to be substantially more than 50%.

### Knock-down of RPTPs produces a deficit in motor axon pathfinding

PTP-$\delta$, PTP-$\sigma$, and PTPRO have been shown to regulate neurite outgrowth *in vitro* (Ledig et al., 1999b; Wang and Bixby, 1999; Q. L. Sun et al., 2000; Stepanek et al., 2001), and expression of putative dominant-negative constructs suggests that PTP-$\delta$ and PTP-$\sigma$ are involved in axon growth and guidance in the visual system (Johnson et al., 2001; Rashid-Doubell et al., 2002). However, the involvement of these RPTPs in developmental axon guidance has not been tested by direct loss-of-function experiments *in vivo*. We used *in ovo* RNAi to examine loss-of-function phenotypes for these RPTPs in motor axon growth.

Embryos were electroporated with dsRNA targeting PTP-$\delta$, PTP-$\sigma$, or PTPRO, and allowed to develop for 48–60 h (to HH 26–27). At HH 24–26, motor axons diverge from the main nerve trunks and grow toward specific muscles (Hamburger, 1975; Op-

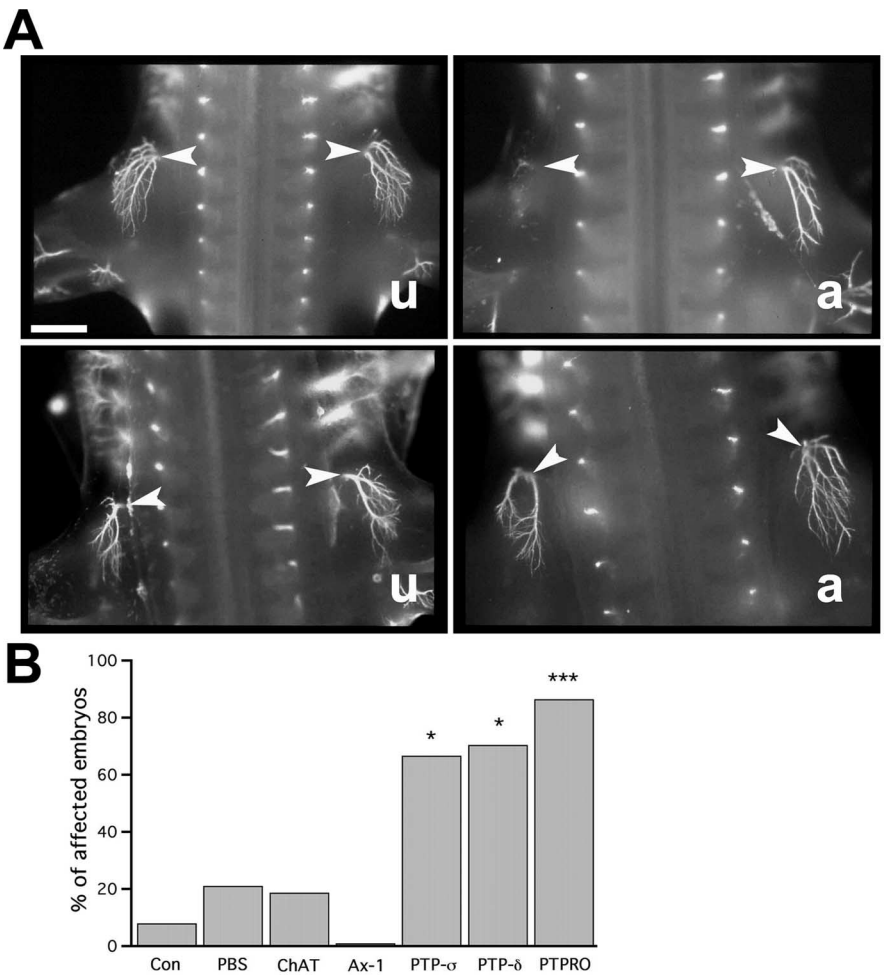


**Figure 4.** Knock-down of RPTPs by *in ovo* RNAi in spinal cord affects the growth of a dorsal nerve in the limb. Spinal cords were electroporated with dsRNA targeting ChAT ($n = 16$), Axonin-1 (Ax-1; $n = 16$), PTP-$\sigma$ ($n = 30$), PTP-$\delta$ ($n = 27$), or PTPRO ($n = 37$) and allowed to develop for 2 d before fixation and fluorescent staining with anti-neurofilament. Control embryos ($n = 25$) were only windowed, and PBS embryos ($n = 19$) were electroporated with PBS. ***A***, Representative photomicrographs showing dorsal views of whole-mount embryos treated with PBS (left 2 panels) or PTPRO dsRNA (right 2 panels). The left (treated) dorsal nerve was visually compared with the right (untreated) dorsal nerve (arrowheads). Embryos were categorized as unaffected (u) or affected (a); affected embryos had much smaller or missing nerves (top), or showed major changes in fasciculation and branching (bottom). Scale bar, 0.5 mm. ***B***, Quantification of dorsal nerve effect. The percentage of affected embryos is shown for each treatment group. Eighty to 100% of control embryos [control (Con), PBS, ChAT, Ax-1] fall into the unaffected category. However, the majority of embryos treated with dsRNA targeting the RPTPs were affected. A two-sided Fisher's exact test was used to compare treatment groups with ChAT. *Significantly different, $p < 0.01$. ***Significantly different, $p < 0.001$. The most severely affected phenotypes (missing or greatly truncated nerves) were never seen with untouched, PBS, ChAT, or axonin-1 embryos; percentages of severely affected embryos were as follows: PTP-$\sigma$, 23%; PTP-$\delta$, 26%; PTPRO, 49% (data not shown).

penheim and Heaton, 1975). To evaluate the growth of peripheral nerves, we examined neurofilament staining in whole mounts of the lumbosacral region of the embryo. RNAi of RPTPs did not grossly affect the major nerve branches in the hindlimb (data not shown). However, knock-down of RPTPs resulted in a conspicuous phenotype in a superficial dorsal nerve (Fig. 4*A*). In control embryos, the untreated and treated nerves had three to four major bundles, with substantial lateral branching. In embryos treated with dsRNA targeting RPTPs, we saw changes in the morphology of this nerve on the treated side. In some cases, there were defasciculation errors such that the nerve had only one or two major bundles, and limited subbranching. In other cases, the nerve was much smaller, seeming to be delayed in its outgrowth, or was missing entirely.

To quantify these effects, we characterized embryos as "affected" (gross differences in the dorsal nerve between treated and untreated sides) or "unaffected" (only minor differences between the two sides) (see Materials and Methods). Approximately 70% of embryos treated with dsRNA targeting either the PTP-$\delta$ or PTP-$\sigma$ were categorized as affected (Fig. 4*B*). Strikingly, >85% of embryos treated with dsRNA targeting the type III RPTP PTPRO were affected (Fig. 4*B*). These results suggest that the function of these RPTPs is essential for proper guidance of the axons in this dorsal nerve.

We used several types of controls to determine the specificity of these effects. As controls for the experimental procedures, we examined embryos in which the egg was windowed but the embryo was left untouched, and embryos injected with PBS and electroporated. We also used controls to determine the specificity of the RNAi itself. First, embryos were electroporated with dsRNA targeting ChAT. ChAT is expressed in motor neurons at this time in development but does not appear to be necessary for initial axon outgrowth to muscle targets (Misgeld et al., 2002). To control for the possibility that interference with any axon guidance cue would produce the phenotype we observed, we electroporated embryos with dsRNA targeting axonin-1. Axonin-1 is expressed in the axons of this dorsal nerve (Fig. 5*A*). The dsRNA we used has been shown to knock down axonin expression and to cause clear and predictable defects in commissural axon pathfinding (Pekarik et al., 2003). In none of the control situations did we observe more than ~20% affected embryos (Figs. 4*B*, 5*B*). Indeed, RNAi for ChAT or axonin-1 produced no increase in affected embryos above that seen for PBS electroporation. Thus, knock-down of RPTPs specifically affects axonal morphology in this dorsal nerve.

To supplement our qualitative categorizations of embryos, we used several quantitative measures of phenotype. A computer algorithm designed to delineate nerve from background (see Materials and Methods) counted pixels in images of each nerve. This gave us an estimate of nerve area, which we used to calculate a ratio of treated nerve area to untreated nerve area (Fig. 6). In control embryos, the mean ratio was slightly larger than 1; in PBS and ChAT embryos, the mean ratio was ~0.9. Embryos electroporated with dsRNA targeting PTP-$\delta$ or PTP-$\sigma$ had a ratio of 0.7. Remarkably, embryos electroporated with dsRNA targeting PTPRO had nerves that were on average only one-half as large as those of controls; this difference was highly statistically significant. Similar results were obtained using the Neurolucida program to calculate total nerve length from traced images. Embryos treated with dsRNA targeting PTPRO had significantly shorter treated nerves than ChAT control embryos ($p < 0.001$); PTP-$\delta$ and PTP-$\sigma$ embryos also showed a decrease

in nerve length on the treated side but were not significantly different from control.

Analysis of nerve branching (number of primary branches on control and treated sides) demonstrated a significant effect of knocking down each of the RPTPs we tested. Embryos treated with dsRNA targeting PTP-$\sigma$ had an average of 3.2 $\pm$ 0.2 primary branches on the untreated side, but only an average of 2.0 $\pm$ 0.2 primary branches on the treated side ($p = 0.0001$; Wilcoxon matched-pairs $t$ test). Embryos treated with dsRNA targeting PTP-$\delta$ or with PTPRO had an average of 2.8 $\pm$ 0.1 primary branches on the untreated sides compared with 2.1 $\pm$ 0.2 and 2.0 $\pm$ 0.2 primary branches on the treated sides, respectively ($p < 0.01$ and $p < 0.001$). In contrast, control embryos treated with dsRNA targeting ChAT had an average of 2.9 $\pm$ 0.2 primary branches on both the untreated and treated side. Overall, our quantitative description of the phenotype followed the same pattern as that of our qualitative data; knock-down of each of the three RPTPs changed the size and morphology of the treated nerve, although interference with PTPRO had the greatest effect in our experiments. These data suggest that type IIa and type III RPTPs are involved in axon pathfinding by chick motor neurons. The effect we saw with PTPRO knock-down represents the first evidence for an *in vivo* role of a type III RPTP in vertebrate axon growth.

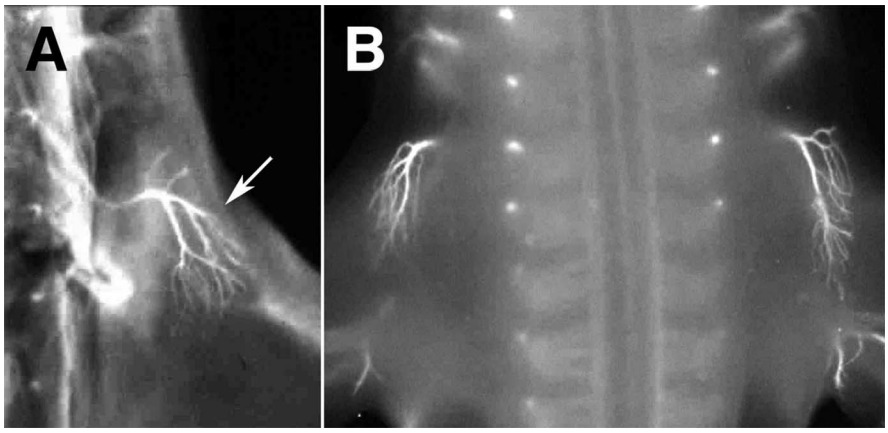


**Figure 5.** Axonin-1 is expressed in the dorsal nerve, but knock-down does not affect outgrowth. ***A***, Dorsal view of an embryo stained with an antibody to axonin-1. The dorsal nerve is axonin-1 positive (arrow). ***B***, Dorsal view of a representative embryo electroporated with dsRNA targeting axonin-1 and stained with anti-neurofilament. The left (treated) nerve has an unaffected phenotype.

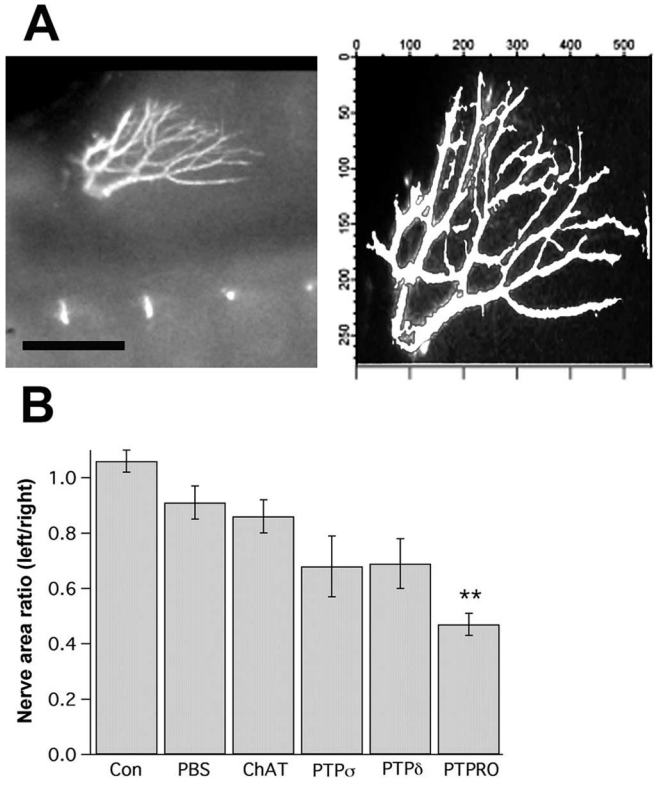


**Figure 6.** Quantification of dorsal nerve phenotype. ***A***, An Igor-based program (see Materials and Methods) was used to calculate the number of pixels contained in the area of the dorsal nerve. The program accurately identified the nerve fascicles; compare the immunostained image (left) (scale bar, 0.5 mm) with the overlay generated by the nerve quantification program (right). ***B***, Nerve areas in electroporated embryos are presented as a ratio of left (treated) nerve area to right [control (Con)] nerve area (mean $\pm$ SEM). There was a tendency for smaller nerves in the embryos treated with PTP-$\sigma$ or PTP-$\delta$ dsRNA; the PTPRO group was significantly smaller than ChAT control embryos. $^{**}p < 0.01$.

**The affected dorsal nerve is the anterior iliotibialis**

To identify the dorsal nerve affected by RPTP knock-down, we followed the projection pattern of this nerve during development by neurofilament staining of embryos at HH 29–32 (E6–E7.5) (data not shown). Over time, the nerve spreads as a thin sheet covering the lateral surface of the thigh. This pattern corresponds to the position of the anterior iliotibialis, a thin, sheet-like muscle that contains both fast- and slow-twitch muscle fibers (Landmesser, 1978a; Milner et al., 1998). To confirm this identification, we used retrograde DiI labeling in E5.5 embryos to identify the neurons of origin of the dorsal nerve. We found that the motor portion of the nerve arises from neurons in the lateral portion of the ventral horn in lumbosacral segments (LS) 1–3 (Fig. 7). This is fully consistent with the position of the anterior iliotibialis motor neuron pool (Landmesser, 1978a). Based on the position and projection pattern of the dorsal nerve, and the position of the motor neurons giving rise to this nerve, we will refer to it as the AITIB. PTPRO mRNA is found in, but is not limited to, neurons of the E5 ventral motor column in which the AITIB motor pool is found (Figs. 1, 7*B*) (data not shown). Thus, PTPRO appears to be expressed in the motor neuron pool that gives rise to the AITIB during the time of AITIB outgrowth. Sensory neurons were also labeled by the retrograde tracing (Fig. 7*B*, inset), showing that the affected AITIB is a mixed nerve.

To examine the effects of RNAi on individual motor axons, we performed anterograde DiI tracing. DiI was placed in the lateral portion of the ventral horn in vibratome sections from LS 1–3 of embryos electroporated with dsRNA targeting PTPRO, and tracing was examined using a confocal microscope. Because of limitations on the thickness of sections suitable for this type of microscopy, the entire length of the AITIB was rarely identified. However, we consistently observed that labeled motor axons on the treated side of the embryo (Fig. 8*A*) were shorter than those on the untreated side of the embryo (*B*). We did not observe differences in motor axon trajectories within the spinal cord or the plexus region. Thus, these experiments indicate that AITIB motor axon growth is retarded by knock-down of PTPRO.

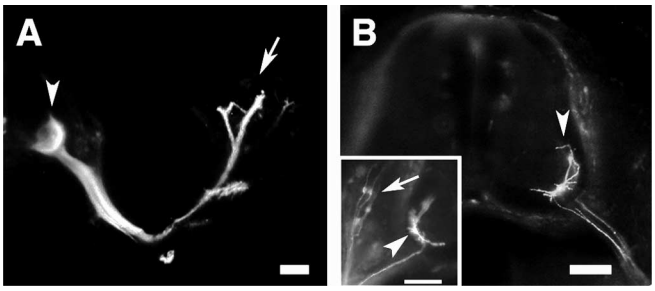


**Figure 7.** The trajectory and origin of the dorsal nerve confirm it as the AITIB nerve. ***A***, Retrograde DiI labeling from the dorsal nerve. Transverse section of the lumbar region of an embryo. The arrow indicates the position of DiI-soaked nitrocellulose pledget placed in the dorsal limb bud in the AITIB termination zone. DiI labels axons extending from neurons in the ventrolateral spinal cord (arrowhead). ***B***, Retrograde labeling from the dorsal nerve labels neurons in the ventrolateral region of the lumbar enlargement. A single neuron is in focus; its axon can be seen leaving the cord, and its dendrites extend some distance medially and laterally (arrowhead). The position of labeled neurons is consistent with the location of the AITIB motor neuron pool (Milner et al., 1998). Inset, In another section, both motor (arrowhead) and sensory (arrow) neurons are labeled by the retrograde tracing. Scale bars, 100 $\mu$m.

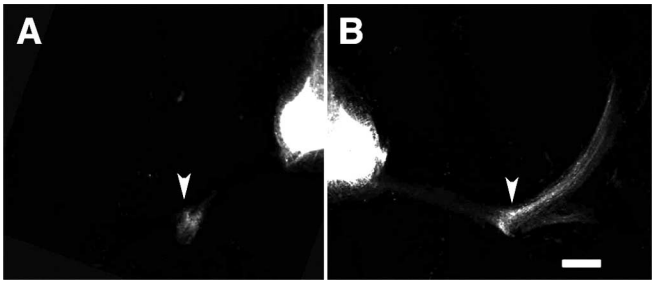


**Figure 8.** Motor axons are shorter when electroporated with dsRNA targeting PTPRO. Confocal images of a 200 $\mu$m section of an embryo treated with PTPRO dsRNA. DiI was placed into the lateral ventral horns of a section from LS 2. Anterograde tracing is apparent in the AITIB at a greater distance from the ventral horn in the untreated side of the embryo (***B***) than in the treated side (***A***). This was a consistent finding after PTPRO knock-down ($n = 6$ embryos) and was not seen with control injections ($n = 7$ embryos). Arrowheads indicate the plexus region where the AITIB turns to grow dorsally. Scale bar, 100 $\mu$m.

### The AITIB phenotype is not caused by increased death of motor neurons

If *in ovo* RNAi of RPTPs led to increased motor neuron death, this could contribute to a reduction in the size of the AITIB. To investigate this possibility, we counted the number of motor neurons in embryos electroporated with PTPRO dsRNA. Serial sections from PTPRO or control embryos were stained with an antibody to the transcription factor Isl-2, an early marker for motor neurons (Tsuchida et al., 1994). Isl-2-positive cells were counted using design-based stereology (see Materials and Methods) in treated and untreated sides of spinal cord lumbosacral segments 1–5. Similar numbers of Isl-2-positive cells in individual sections were seen in both PTPRO RNAi embryos and in controls (Fig. 9). Additionally, the estimates of total motor neurons in the entire volume examined were similar between the two sides of the embryos. The ratio of Isl-2-positive cells in treated compared with untreated spinal cord halves was $0.98 \pm 0.02$ for control embryos, and $0.99 \pm 0.01$ for PTPRO RNAi embryos ($n = 3$ for both groups). Thus, cell death of motor neurons does not contribute substantially to the mean 50% decrease in AITIB size in PTPRO-targeted embryos.

### Combinatorial RNAi: evidence for competition between type IIa and type III RPTPs

Experiments in *Drosophila* have shown that type IIa and type III RPTPs can cooperate or compete in the guidance of both central axon fascicles and peripheral motor axons (Desai et al., 1997; Q. Sun et al., 2000; Schindelholz et al., 2001). Do vertebrate RPTPs also interact in the regulation of motor axon pathfinding? To answer this question, we used combinatorial RNAi. It has been demonstrated that several genes can be silenced together by injecting a combination of dsRNAs targeting the genes of interest, if the RNAs are injected at reasonably high concentrations (Schmid et al., 2002). For our experiments, we first determined that 500 ng/$\mu$l was the dsRNA concentration that produced the most reliable PTPRO phenotype (data not shown). In the combination experiments, we therefore used all of the dsRNAs at a final concentration of 500 ng/$\mu$l.

Embryos in which both type IIa RPTPs (PTP-$\delta$ and PTP-$\sigma$) were targeted had approximately the same severity of phenotypes as embryos in which either PTP-$\delta$ or PTP-$\sigma$ alone were targeted, although the percentage affected was slightly higher in the combination experiments than for either RPTP alone (Fig. 10*A*). These data provide no evidence for a strong interaction between PTP-$\delta$ and PTP-$\sigma$ in the growth of the AITIB.

Embryos in which either PTP-$\delta$ or PTP-$\sigma$ was targeted concomitantly with the type III RPTP, PTPRO, were on average less severely affected than embryos in which PTPRO alone was targeted (Fig. 10*B*). In the case of PTPRO/PTP-$\delta$, only 50% of embryos were classified as affected, compared with 87% for PTPRO alone, a significant reduction ($p < 0.01$). To ensure that this reduction in phenotype severity was not simply attributable to addition of a second dsRNA, we used a combination of PTPRO and ChAT dsRNAs. A slight and nonsignificant reduction in the percentage of affected embryos was seen in this case, indicating that the reduction in phenotype severity seen with PTPRO/PTP-$\delta$ was specific to this combination. These data suggest that PTPRO and PTP-$\delta$ compete functionally during the growth of the AITIB nerve. A similar trend was seen for PTP-$\sigma$/PTPRO, but the data do not allow a conclusion in this case.

Finally, we tested a combination of dsRNAs targeting all three RPTPs (Fig. 10*C*). In this case, the reversion of the PTPRO phenotype was even more dramatic, with only 41% of the embryos categorized as affected ($p < 0.01$). As a control for the use of large amounts of dsRNA, we tested PTPRO dsRNA in conjunction with 1000 ng/$\mu$l ChAT dsRNA; no significant difference was seen compared with PTPRO alone. These data suggest that PTP-$\delta$, together with PTP-$\sigma$, counteracts the role of PTPRO in controlling the outgrowth of the AITIB. The need to balance the functional activities of type IIa and type III RPTPs in motor axon guidance is similar to the situation in *Drosophila*. The data may indicate a conserved function for RPTPs in motor axon outgrowth from flies to vertebrates.

## Discussion

RNAi targeting of PTP-$\delta$, PTP-$\sigma$, or PTPRO in spinal motor neurons led to dramatic changes in the morphology of the developing AITIB nerve. Although RNAi produced similar changes for all of the RPTPs examined, knock-down of the type III RPTP PTPRO produced the strongest effects. Knock-down of the type IIa RPTPs in combination with PTPRO suggests competition among these RPTPs in axon guidance. Notably, our results provide the first evidence implicating a type III RPTP in vertebrate axon pathfinding.

RPTPs could be acting at several places to regulate outgrowth of AITIB axons. Embryos lacking AITIB nerves suggest involvement of RPTPs in axon initiation or spinal nerve exiting. Alternatively, RPTPs could function at choice points along axonal pathways; loss of RPTP function could cause axons to stall or make incorrect decisions. In *Drosophila*, loss-of-function mutants of type IIa RPTPs exhibit "stall" or "stop short" phenotypes in motor axon fascicles (Desai et al., 1996; Desai et al., 1997). As in these mutants, phenotypes in our RPTP RNAi embryos varied considerably. We cannot determine whether this phenotypic variation is attributable to incomplete "penetrance" or variation in the efficacy of the RNAi, but incomplete penetrance has been observed in many cases for *Drosophila* RPTPs.

Retrograde tracing from the AITIB also labeled sensory neurons. Thus, the affected nerve contains sensory fibers. It is unlikely that our electroporation targeted sensory neurons, because we found transfection of sensory ganglia only when we electroporated before HH 18. Our phenotypic analysis suggests that the whole nerve is affected by RPTP dsRNA electroporation, including the sensory component. This finding is consistent with a body of evidence linking sensory axon pathfinding to decisions made by earlier-extending motor axons (Honig et al., 1986; Landmesser and Honig, 1986; Scott, 1986; Wang and Scott, 1997; Honig et al., 1998).

The RPTP knock-down phenotypes also included gross changes in fasciculation pattern. Some embryos exhibited phenotypes in which primary or secondary branches of the nerves appeared to be fused together in the treated side. In some cases, secondary and tertiary branches developed more distally in the treated AITIB than in the control AITIB. These phenotypes implicate RPTPs, and particularly PTPRO, in defasciculation. The *Drosophila* PTPRO relative DPTP10D is involved in defasciculation of the intersegmental nerve b, along with other RPTPs (Sun et al., 2001).

RPTPs likely act both as ligands and as receptors, and the effects we observe may be attributable to loss of either or both functions. Proper guidance of photoreceptor cell axons in *Drosophila*, for example, is dependent on both cell-autonomous (presumably receptor) functions of RPTPs, as well as non-cell-autonomous (presumably ligand) functions (Garrity et al., 1999; Clandinin et al., 2001; Maurel-Zaffran et al., 2001). Additionally, RPTPs might act in *cis* to regulate other guidance molecule-receptor interactions within the axon or on growth cones. The *Caenorhabditis elegans* RPTP Clr-1, for example, inhibits signaling in *cis* through the netrin receptor UNC40 (Chang et al., 2004). In the spinal cord, effects of RNAi could be attributable to loss of RPTPs as receptors on AITIB motor neurons, making the neurons unresponsive to growth-promoting factors. Effects could also be attributable to loss of RPTPs from other cells, so that receptors on the AITIB are not activated by their growth-promoting ligands. In the spinal nerves and crural plexus, RPTPs could also be acting autonomously within the AITIB axons, or could be signaling the AITIB axons from neighboring nerve fibers. Once in the limb, changes in AITIB morphology would presumably be attributable to cell-autonomous RPTP action.

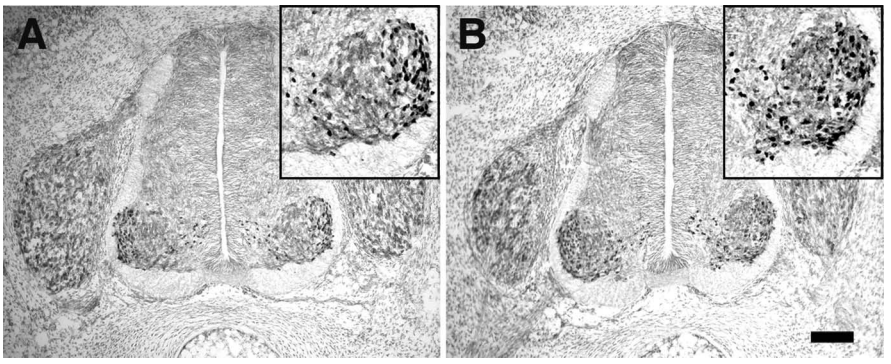


**Figure 9.** dsRNA electroporation does not cause motor neuron cell death. Treated and control embryos were dissected at E5, and sections were stained with Islet-2 antibody to identify motor neurons of the lateral motor column. LS 2 spinal cord sections of untouched embryos (***A***) and dsPTPRO RNA-treated embryos (***B***) have the same gross morphology and have the same density of cells immunopositive for Islet-2 (see insets). Scale bar, 100 $\mu$m.

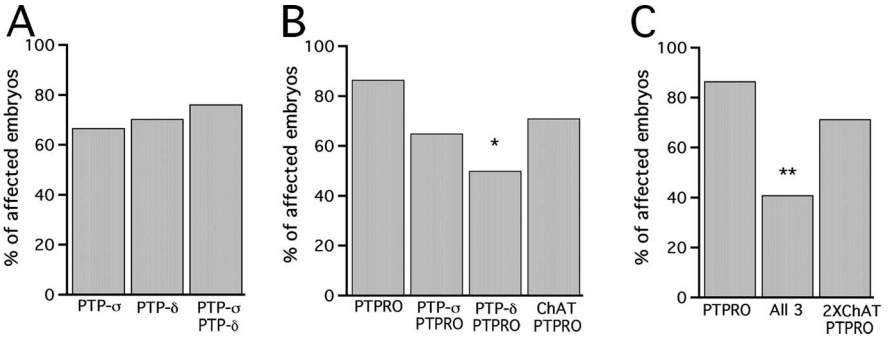


**Figure 10.** Targeting of multiple RPTPs suggests complex interactions in axon growth. Embryos were treated with dsRNA targeted to the indicated RPTPs. Embryos were examined as whole mounts and categorized as unaffected or affected. ***A***, Simultaneous targeting of PTP-$\sigma$ and PTP-$\delta$ ($n = 21$) produced no significant change in the number of affected embryos compared with PTP-$\sigma$ or PTP-$\delta$ alone. ***B***, Simultaneous targeting of PTP-$\delta$ and PTPRO ($n = 20$) produced significantly fewer affected embryos than PTPRO alone ( $p < 0.01$; Fisher's exact test). Simultaneous targeting of PTP-$\sigma$ and PTPRO ($n = 20$), or of ChAT and PTPRO ($n = 24$), produced no significant change in the number of affected embryos compared with PTPRO alone. ***C***, Simultaneous targeting of PTP-$\sigma$, PTP-$\delta$, and PTPRO ($n = 22$) reduced the percentage of affected embryos to less than one-half that seen by targeting PTPRO alone ( $p < 0.001$; Fisher's exact test). Control experiments in which PTPRO was combined with a 2× concentration of dsChAT RNA ($n = 21$) produced no significant change in the number of affected embryos compared with PTPRO alone, indicating that the effect of the RPTP knock-down is specific and not attributable to dilution of PTPRO dsRNA by other dsRNA.

Interpretation of these knock-down experiments is complicated by our limited understanding of the binding partners of RPTPs and their effects on RPTP function. PTP-$\delta$ binds homophilically (Wang and Bixby, 1999), although it may have other partners. PTP-$\sigma$ binds to heparan sulfate proteoglycans and to other uncharacterized ligands in retinal basement membranes (Ledig et al., 1999b; Aricescu et al., 2002). The binding partners of PTPRO are unknown, although it is unlikely to bind homophilically (Stepanek et al., 2001).

It is difficult to predict effects of RPTP knock-down on motor axon growth from available data. Because PTP-$\delta$ promotes neurite outgrowth *in vitro*, and putative dominant-negative mutants of PTP-$\delta$ cause decreased growth of retinotectal axons (Johnson et al., 2001), one might expect the removal of PTP-$\delta$ to cause a decrease in size of the nerve. Knock-down of PTP-$\delta$ indeed de-

creased some aspects of AITIB growth. In contrast, available evidence suggests that unliganded PTP-$\sigma$ is inhibitory to axon growth, and that ligand binding may promote growth by inactivating PTP-$\sigma$ (Ledig et al., 1999b; Johnson et al., 2001). Consistent with this idea, loss of PTP-$\sigma$ function accelerates regeneration of adult peripheral nerves (McLean et al., 2002). In our experiments, however, knock-down of PTP-$\sigma$ alone did not appear to increase nerve growth. It is possible that PTP-$\sigma$ has distinct functions in different axonal populations. Alternatively, ligand rather than receptor functions may be important. The situation for PTPRO is even less clear. Although the extracellular domain of PTPRO is neurite inhibitory *in vitro* (Stepanek et al., 2001), effects of PTPRO as a receptor in PTPRO-expressing neurons have not been studied.

Although the three RPTPs we tested appear to have distinct activities *in vitro*, the gross phenotypes caused by single knockdowns in motor neurons were similar. Because there is no exacerbation of the single-knock-down phenotypes in embryos treated with dsRNA targeting PTP-$\delta$ and PTP-$\sigma$, these RPTPs might have partially redundant functions in regulating the outgrowth of the AITIB. However, double- and triple-combination experiments indicate a functional competition between PTPRO and the type IIa RPTPs in AITIB growth. This unexpected complexity is likely to be partially attributable to our level of analysis. It is clear that functional interactions among RPTPs cannot be reliably predicted on the basis of observations of gross phenotypes of single null mutants (Krueger et al., 1996; Desai et al., 1997; Schindelholz et al., 2001; Sun et al., 2001).

At what level are these RPTPs interacting to regulate axon growth? There is no indication thus far that any RPTPs share the same ligands or receptors, although LAR, PTP-$\delta$, and PTP-$\sigma$ do share potential heparan sulfate proteoglycan binding motifs (Aricescu et al., 2002; Johnson and Van Vactor, 2003). It seems more likely that the RPTPs are interacting downstream of ligand–receptor interactions. Little is known about neuronal substrates for these RPTPs. PTP-$\delta$, PTP-$\sigma$, and LAR bind to the liprin protein family, which is implicated in several aspects of synapse formation (Serra-Pages et al., 1995; Zhen and Jin, 1999; Kaufmann et al., 2002; Wyszynski et al., 2002). Substrates for PTPRO may include Trk receptors (Beltran et al., 2003), in addition to the novel neural protein NPCD (neuronal pentraxin with chromo domain) (Chen and Bixby, 2005a,b). More progress has been made in the discovery of potential substrates for LAR; it can act together with Abl to coordinate phosphorylation/dephosphorylation of the profilin-interacting protein Ena. Additionally, LAR interacts with the guanine nucleotide exchange factor Trio, which can activate Rho family GTPases to regulate actin filaments (Bixby, 2001; Johnson and Van Vactor, 2003). A recent paper shows that PTP-$\delta$ interacts with an actin-binding protein called MIM in fibroblasts, suggesting that cytoskeletal interactions are common to type IIa RPTPs (Gonzalez-Quevedo et al., 2005). The type IIa and type III RPTPs could have opposing effects on the same signaling pathway, or affect opposing signaling pathways, to control cytoskeletal rearrangements in the growth cone.

It is surprising that the axon pathfinding defects we saw with RPTP knock-down were confined to the AITIB. PTP-$\delta$, PTP-$\sigma$, and PTPRO are expressed in many ventrolateral neurons throughout the length of the lumbosacral spinal cord. Based on GFP transfection experiments, we produce efficient electroporation in 7–10 segments of the cord, in both medial and lateral cells. Thus, it does not seem likely that the dsRNA is selectively entering the AITIB motor pool. Our PTPRO–GFP experiments do not provide evidence for selective efficacy of RNAi in different cell populations. Possible explanations for the apparent selectivity include the following: (1) lower baseline levels of RPTP expression in AITIB neurons, (2) lack of neighboring axon bundles in the AITIB pathway to provide guidance cues, and (3) the timing of growth relative to knock-down—the AITIB emerges precociously compared with other nerves from the crural plexus. The isolation of the AITIB from other nerves may also play another role. Perhaps pathfinding is disrupted in other axon fascicles, but cannot be observed against a background of normal axons with the assessment techniques we used.

The accessibility of chick spinal motor neurons combined with the ability to perform RNAi with long dsRNAs has allowed us to perform direct loss-of-function experiments with several RPTPs in developing projection neurons. The strongest pathfinding defects were seen by targeting the type III RPTP, PTPRO. Our data also support the idea of competition and cooperation between type IIa and type III RPTPs in regulating vertebrate axon guidance, suggesting an evolutionary conservation of RPTP function. Among the major challenges remaining is the identification of extracellular and intracellular binding partners of these RPTPs, providing insight into the mechanisms underlying RPTP function in axonal pathfinding.

## References


Aricescu AR, McKinnell IW, Halfter W, Stoker AW (2002) Heparan sulfate proteoglycans are ligands for receptor protein tyrosine phosphatase sigma. Mol Cell Biol 22:1881–1892.

Beltran PJ, Bixby JL, Masters BA (2003) Expression of PTPRO during mouse development suggests involvement in axonogenesis and differentiation of NT-3 and NGF-dependent neurons. J Comp Neurol 456:384–395.

Bixby JL (2000) Receptor tyrosine phosphatases in axon growth and guidance. NeuroReport 11:R5–R10.

Bixby JL (2001) Ligands and signaling through receptor-type tyrosine phosphatases. IUBMB Life 51:157–163.

Bixby JL, Jhabvala P (1990) Extracellular matrix molecules and cell adhesion molecules induce neurites through different mechanisms. J Cell Biol 111:2725–2732.

Bodden K, Bixby JL (1996) CRYP-2: a receptor-type tyrosine phosphatase selectively expressed by developing vertebrate neurons. J Neurobiol 31:309–324.

Bron R, Eickholt BJ, Vermeren M, Fragale N, Cohen J (2004) Functional knockdown of neuropilin-1 in the developing chick nervous system by siRNA hairpins phenocopies genetic ablation in the mouse. Dev Dyn 230:299–308.

Chang C, Yu TW, Bargmann CI, Tessier-Lavigne M (2004) Inhibition of netrin-mediated axon attraction by a receptor protein tyrosine phosphatase. Science 305:103–106.

Chen B, Bixby JL (2005a) Neuronal pentraxin with chromo domain (NPCD) is a novel class of protein expressed in multiple neuronal domains. J Comp Neurol 481:391–402.

Chen B, Bixby JL (2005b) A novel substrate of receptor tyrosine phosphatase PTPRO is required for nerve growth factor-induced process outgrowth. J Neurosci 25:880–888.

Chilton JK, Stoker AW (2000) Expression of receptor protein tyrosine phosphatases in embryonic chick spinal cord. Mol Cell Neurosci 16:470–480.

Clandinin TR, Lee CH, Herman T, Lee RC, Yang AY, Ovasapyan S, Zipursky SL (2001) *Drosophila* LAR regulates R1–R6 and R7 target specificity in the visual system. Neuron 32:237–248.

Desai CJ, Gindhart Jr JG, Goldstein LS, Zinn K (1996) Receptor tyrosine phosphatases are required for motor axon guidance in the *Drosophila* embryo. Cell 84:599–609.

Desai CJ, Krueger NX, Saito H, Zinn K (1997) Competition and cooperation among receptor tyrosine phosphatases control motoneuron growth cone guidance in *Drosophila*. Development 124:1941–1952.

Elbashir SM, Martinez J, Patkaniowska A, Lendeckel W, Tuschl T (2001) Functional anatomy of siRNAs for mediating efficient RNAi in *Drosophila melanogaster* embryo lysate. EMBO J 20:6877–6888.

Elchebly M, Wagner J, Kennedy TE, Lanctot C, Michaliszyn E, Itie A, Drouin J, Tremblay ML (1999) Neuroendocrine dysplasia in mice lacking protein tyrosine phosphatase sigma. Nat Genet 21:330–333.

Garrity PA, Lee CH, Salecker I, Robertson HC, Desai CJ, Zinn K, Zipursky SL (1999) Retinal axon target selection in *Drosophila* is regulated by a receptor protein tyrosine phosphatase. Neuron 22:707–717.

Gonzalez-Quevedo R, Shoffer M, Horng L, Oro AE (2005) Receptor tyrosine phosphatase-dependent cytoskeletal remodeling by the hedgehog-responsive gene MIM/BEG4. J Cell Biol 168:453–463.

Hamburger V (1975) Cell death in the development of the lateral motor column of the chick embryo. J Comp Neurol 160:535–546.

Holen T, Amarzguioui M, Wiiger MT, Babaie E, Prydz H (2002) Positional effects of short interfering RNAs targeting the human coagulation trigger Tissue Factor. Nucleic Acids Res 30:1757–1766.

Honig MG, Lance-Jones C, Landmesser L (1986) The development of sensory projection patterns in embryonic chick hindlimb under experimental conditions. Dev Biol 118:532–548.

Honig MG, Petersen GG, Rutishauser US, Camilli SJ (1998) *In vitro* studies of growth cone behavior support a role for fasciculation mediated by cell adhesion molecules in sensory axon guidance during development. Dev Biol 204:317–326.

Johnson KG, Van Vactor D (2003) Receptor protein tyrosine phosphatases in nervous system development. Physiol Rev 83:1–24.

Johnson KG, McKinnell IW, Stoker AW, Holt CE (2001) Receptor protein tyrosine phosphatases regulate retinal ganglion cell axon outgrowth in the developing *Xenopus* visual system. J Neurobiol 49:99–117.

Kaufmann N, DeProto J, Ranjan R, Wan H, Van Vactor D (2002) *Drosophila* liprin-$\alpha$ and the receptor phosphatase Dlar control synapse morphogenesis. Neuron 34:27–38.

Krueger NX, Van Vactor D, Wan HI, Gelbart WM, Goodman CS, Saito H (1996) The transmembrane tyrosine phosphatase DLAR controls motor axon guidance in *Drosophila*. Cell 84:611–622.

Lance-Jones C, Landmesser L (1981) Pathway selection by chick lumbosacral motoneurons during normal development. Proc R Soc Lond B Biol Sci 214:1–18.

Landmesser L (1978a) The distribution of motoneurones supplying chick hind limb muscles. J Physiol (Lond) 284:371–389.

Landmesser L (1978b) The development of motor projection patterns in the chick hind limb. J Physiol (Lond) 284:391–414.

Landmesser L, Honig MG (1986) Altered sensory projections in the chick hind limb following the early removal of motoneurons. Dev Biol 118:511–531.

Ledig MM, McKinnell IW, Mrsic-Flogel T, Wang J, Alvares C, Mason I, Bixby JL, Mueller BK, Stoker AW (1999a) Expression of receptor tyrosine phosphatases during development of the retinotectal projection of the chick. J Neurobiol 39:81–96.

Ledig MM, Haj F, Bixby JL, Stoker AW, Mueller BK (1999b) The receptor tyrosine phosphatase CRYP$\alpha$ promotes intraretinal axon growth. J Cell Biol 147:375–388.

Lemmon V, McLoon SC (1986) The appearance of an L1-like molecule in the chick primary visual pathway. J Neurosci 6:2987–2994.

Maurel-Zaffran C, Suzuki T, Gahmon G, Treisman JE, Dickson BJ (2001) Cell-autonomous and -nonautonomous functions of LAR in R7 photoreceptor axon targeting. Neuron 32:225–235.

McLean J, Batt J, Doering LC, Rotin D, Bain JR (2002) Enhanced rate of nerve regeneration and directional errors after sciatic nerve injury in receptor protein tyrosine phosphatase sigma knock-out mice. J Neurosci 22:5481–5491.

Milner LD, Rafuse VF, Landmesser LT (1998) Selective fasciculation and divergent pathfinding decisions of embryonic chick motor axons projecting to fast and slow muscle regions. J Neurosci 18:3297–3313.

Misgeld T, Burgess RW, Lewis RM, Cunningham JM, Lichtman JW, Sanes JR (2002) Roles of neurotransmitter in synapse formation: development of neuromuscular junctions lacking choline acetyltransferase. Neuron 36:635–648.

Newsome TP, Asling B, Dickson BJ (2000) Analysis of *Drosophila* photoreceptor axon guidance in eye-specific mosaics. Development 127:851–860.

Oppenheim RW, Heaton MB (1975) The retrograde transport of horseradish peroxidase from the developing limb of the chick embryo. Brain Res 98:291–302.

Pekarik V, Bourikas D, Miglino N, Joset P, Preiswerk S, Stoeckli ET (2003) Screening for gene function in chicken embryo using RNAi and electroporation. Nat Biotechnol 21:93–96.

Rashid-Doubell F, McKinnell I, Aricescu AR, Sajnani G, Stoker A (2002) Chick PTP$\sigma$ regulates the targeting of retinal axons within the optic tectum. J Neurosci 22:5024–5033.

Schaeren-Wiemers N, Gerfin-Moser A (1993) A single protocol to detect transcripts of various types and expression levels in neural tissue and cultured cells: *in situ* hybridization using digoxigenin-labelled cRNA probes. Histochemistry 100:431–440.

Schindelholz B, Knirr M, Warrior R, Zinn K (2001) Regulation of CNS and motor axon guidance in *Drosophila* by the receptor tyrosine phosphatase DPTP52F. Development 128:4371–4382.

Schmid A, Schindelholz B, Zinn K (2002) Combinatorial RNAi: a method for evaluating the functions of gene families in *Drosophila*. Trends Neurosci 25:71–74.

Scott SA (1986) Skin sensory innervation patterns in embryonic chick hindlimb following dorsal root ganglion reversals. J Neurobiol 17:649–668.

Serra-Pages C, Kedersha NL, Fazikas L, Medley Q, Debant A, Streuli M (1995) The LAR transmembrane protein tyrosine phosphatase and a coiled-coil LAR-interacting protein co-localize at focal adhesions. EMBO J 14:2827–2838.

Sommer L, Rao M, Anderson DJ (1997) RPTP $\delta$ and the novel protein tyrosine phosphatase RPTP $\psi$ are expressed in restricted regions of the developing central nervous system. Dev Dyn 208:48–61.

Stepanek L, Sun QL, Wang J, Wang C, Bixby JL (2001) CRYP-2/cPTPRO is a neurite inhibitory repulsive guidance cue for retinal neurons in vitro. J Cell Biol 154:867–878.

Stoeckli ET, Landmesser LT (1995) Axonin-1, Nr-CAM, and Ng-CAM play different roles in the in vivo guidance of chick commissural neurons. Neuron 14:1165–1179.

Stoker AW, Gehrig B, Haj F, Bay BH (1995) Axonal localisation of the CAM-like tyrosine phosphatase CRYP $\alpha$: a signalling molecule of embryonic growth cones. Development 121:1833–1844.

Sun Q, Bahri S, Schmid A, Chia W, Zinn K (2000) Receptor tyrosine phosphatases regulate axon guidance across the midline of the *Drosophila* embryo. Development 127:801–812.

Sun Q, Schindelholz B, Knirr M, Schmid A, Zinn K (2001) Complex genetic interactions among four receptor tyrosine phosphatases regulate axon guidance in *Drosophila*. Mol Cell Neurosci 17:274–291.

Sun QL, Wang J, Bookman RJ, Bixby JL (2000) Growth cone steering by receptor tyrosine phosphatase $\delta$ defines a distinct class of guidance cue. Mol Cell Neurosci 16:686–695.

Thompson KM, Uetani N, Manitt C, Elchebly M, Tremblay ML, Kennedy TE (2003) Receptor protein tyrosine phosphatase $\sigma$ inhibits axonal regeneration and the rate of axon extension. Mol Cell Neurosci 23:681–692.

Tosney KW, Landmesser LT (1985) Specificity of early motoneuron growth cone outgrowth in the chick embryo. J Neurosci 5:2336–2344.

Tsuchida T, Ensini M, Morton SB, Baldassare M, Edlund T, Jessell TM, Pfaff SL (1994) Topographic organization of embryonic motor neurons defined by expression of LIM homeobox genes. Cell 79:957–970.

Uetani N, Kato K, Ogura H, Mizuno K, Kawano K, Mikoshiba K, Yakura H, Asano M, Iwakura Y (2000) Impaired learning with enhanced hippocampal long-term potentiation in PTP$\delta$-deficient mice. EMBO J 19:2775–2785.

Van der Zee CE, Man TY, Van Lieshout EM, Van der Heijden I, Van Bree M, Hendriks WJ (2003) Delayed peripheral nerve regeneration and central nervous system collateral sprouting in leucocyte common antigen-related protein tyrosine phosphatase-deficient mice. Eur J Neurosci 17:991–1005.

Van Vactor D, O'Reilly AM, Neel BG (1998) Genetic analysis of protein tyrosine phosphatases. Curr Opin Genet Dev 8:112–126.

Wallace MJ, Batt J, Fladd CA, Henderson JT, Skarnes W, Rotin D (1999) Neuronal defects and posterior pituitary hypoplasia in mice lacking the receptor tyrosine phosphatase PTP$\sigma$. Nat Genet 21:334–338.

Wang G, Scott SA (1997) Muscle sensory innervation patterns in embryonic chick hindlimbs following dorsal root ganglion reversal. Dev Biol 186:27–35.

Wang J, Bixby JL (1999) Receptor tyrosine phosphatase-$\delta$ is a homophilic,

neurite-promoting cell adhesion molecular for CNS neurons. Mol Cell Neurosci 14:370–384.

Wyszynski M, Kim E, Dunah AW, Passafaro M, Valtschanoff JG, Serra-Pages C, Streuli M, Weinberg RJ, Sheng M (2002) Interaction between GRIP and liprin-α/SYD2 is required for AMPA receptor targeting. Neuron 34:39–52.

Xie Y, Yeo TT, Zhang C, Yang T, Tisi MA, Massa SM, Longo FM (2001) The leukocyte common antigen-related protein tyrosine phosphatase receptor regulates regenerative neurite outgrowth *in vivo*. J Neurosci 21:5130–5138.

Yan H, Grossman A, Wang H, D'Eustachio P, Mossie K, Musacchio JM, Silvennoinen O, Schlessinger J (1993) A novel receptor tyrosine phosphatase-σ that is highly expressed in the nervous system. J Biol Chem 268:24880–24886.

Yang T, Bernabeu R, Xie Y, Zhang JS, Massa SM, Rempel HC, Longo FM (2003) Leukocyte antigen-related protein tyrosine phosphatase receptor: a small ectodomain isoform functions as a homophilic ligand and promotes neurite outgrowth. J Neurosci 23:3353–3363.

Yeo TT, Yang T, Massa SM, Zhang JS, Honkaniemi J, Butcher LL, Longo FM (1997) Deficient LAR expression decreases basal forebrain cholinergic neuronal size and hippocampal cholinergic innervation. J Neurosci Res 47:348–360.

Zhen M, Jin Y (1999) The liprin protein SYD-2 regulates the differentiation of presynaptic termini in *C. elegans*. Nature 401:371–375.